DE GRUYTER OPEN

DOI: 10.1515/ace-2015-0103

ARCHIVES OF CIVIL ENGINEERING
Vol. LXII ISSUE 4, Part 1 2016

MECHANISM OF FATIGUE CRACK GROWTH OF BRIDGE STEEL STRUCTURES

H. ZHU[1]

This study was carried out on the background of Sutong Bridge project based on fracture mechanics, aiming at analyzing the growth mechanism of fatigue cracks of a bridge under the load of vehicles. Stress intensity factor (SIF) can be calculated by various methods. Three steel plates with different kinds of cracks were taken as the samples in this study. With the combination of finite element analysis software ABAQUS and the J integral method, SIF values of the samples were calculated. After that, the extended finite element method in the simulation of fatigue crack growth was introduced, and the simulation of crack growth paths under different external loads was analyzed. At last, we took a partial model from the Sutong Bridge and supposed its two dangerous parts already had fine cracks; then simulative vehicle load was added onto the U-rib to predict crack growth paths using the extended finite element method.

Keywords: Stress intensity factor, extended finite element method, simulation of fatigue crack growth, bridge

1. INTRODUCTION

In most practical engineering problems, loads on structures are not fixed but change in size and direction over time. Fine cracks can appear on steel structures under the long-term load effect [1-2], thus cracks can gradually extend over time without examination and maintenance till the whole component completely fractures. With the development of technology, the application of metal materials to engineering is irreplaceable; however, it also brings disastrous accidents.

[1] Master, College of Civil Engineering, Campus on Avenue Hope, Yancheng Institute of Technology, Yancheng, Jiangsu, 224051, Chin, e-mail: zhuhuazh2233@163.com

Fracture mechanics mainly developed in late 1920's. In 1921, a landmark research on facture theories of fragile materials was carried out by Griffith [3-4], who also put forward hypotheses about unstable growth of cracks.

Paris formula, the most commonly used formula in determining growth rates of fatigue cracks at present, involves an important parameter, i.e., the stress intensity factor (SIF) of the crack tips [5]. Currently there are various kinds of methods of calculating the K value of SIF, such as stress function [6], integral transformation [7], finite element method [8], boundary element method [9] and boundary collocation method, etc. In China, many scholars explored SIF through experiments and finite element simulation. For example, the finite element simulation on SIF of semi-oval surface cracks was carried out by Dao N H et al. [11]. Dazhao YU et al. [12] simulated cracks on screw joints of airplanes using finite element simulation. Overseas, great results of finite element simulation of fracture parameters have been achieved. For example, Ayhan. A et al. [13] simulated SIF of three-dimensional mixed-mode cracks in functionally graded materials by using the finite element general software FGMC3D as well as the enriched finite element method. Peng.Y et al. [14] deduced and solved the SIF theoretical formula of semi-oval surface cracks. In the meantime, current finite element simulation methods for crack growth problems are varied, and commonly used finite element software include ANSYS, ABAQUS and FRANC3D, etc. Sukumar N [15] used the extended finite element method to simulate the displacement field of crack tips and discontinuous components; besides, he combined the fast calculation method with the Paris formula of crack growth to forecast the crack front. On the basis of Paris formula, Đurđević A et al. [16] successfully simulated growth paths of two-dimensional plane cracks. Based on the above facts, this study took Sutong Bridge as the research object to study the mechanism of fatigue crack growth of bridge steel structures.

2. CALCULATION OF STRESS INTENSITY FACTOR USING J-INTEGRAL METHOD

2.1. J-INTEGRAL METHOD

J-integral is a stress-strain parameter that characterizes the energy, which can be measured by simple and reliable experiments [17]. J integral can be used to characterize the energy release during crack growth [18], and the paths of integration are curves surround the crack front. The start point and the end point are at two surfaces of the crack respectively, which are conserved integrals unrelated to paths. J integral has conservativeness, thus the calculation accuracy of the crack tip stress can be

improved by choosing integral loops that are away from the crack tip. The calculation formula is as follow:

$$J = \int_{\Gamma} w dy - \int_{\Gamma} \left(t_x \frac{\partial u_x}{\partial x} + t_y \frac{\partial u_y}{\partial y} \right) ds \tag{2.1}$$

where:

Γ – a random path surrounds the crack tip;, w – the strain-energy density (i.e., the strain energy of unit volume), tx – the gravity vector along the x axis, ty – the gravity vector along the y axis, S – the distance along Γ, ux – the displacement component of x axis, uy – the displacement component of y axis, n – the unit outer normal vector of paths. In consideration of the tubular planes of crack tips, J-integral theories can be applied to three-dimensional problems using the divergence theorem. In ABAQUS, integral paths of J-integral method can be considered automatically. SIF can be determined through calculating J-integral values along the crack surface paths.

In calculation of SIF KI, the J-integral method and the virtual crack closure method have higher computational accuracy compared with the displacement correlation method. Generally, errors of the J-integral method and the virtual crack closure method decrease with the increase of a/b value, while the error of displacement correlation method increases with the increase of a/b value. The following three equations are used for calculation of center cracks, single-edge cracks and double-edge cracks respectively.

$$K_I = F\sigma\sqrt{\pi\alpha} = \left[1 - 0.5\frac{a}{b} + 0.326\left(\frac{a}{b}\right)^2\right]\frac{\sigma\sqrt{\pi\alpha}}{1-\frac{a}{b}} \tag{2.2}$$

$$K_I = F\sigma\sqrt{\pi\alpha} = \left[1.12 - 0.23\frac{a}{b} + 10.6\left(\frac{a}{b}\right)^2 - 21.7\left(\frac{a}{b}\right)^2 + 30.4\left(\frac{a}{b}\right)^4\right]\sigma\sqrt{\pi\alpha} \tag{2.3}$$

$$K_I = F\sigma\sqrt{\pi\alpha} = \left[1.12 + 0.41\frac{a}{2b} - 4.78\left(\frac{a}{2b}\right)^2 + 15.44\left(\frac{a}{2b}\right)^2\right]\sigma\sqrt{\pi\alpha} \tag{2.4}$$

2.2. EXAMPLE ANALYSIS OF STEEL CRACKS

2.2.1. SELECTION OF OBJECTS AND CRACKS

This study took steel plates as samples and used finite element analysis software ABAQUS for analysis. The size of selected steel plates was scaled down according to the size of steel plates of Sutong Bridge, which was 2b=500 mm and 2h=1000 mm. Considering that positions of cracks could affect the analysis results, cracks in three different forms were selected (as shown in Fig. 1).

Center crack (2a=10 mm) had two tips; due to the symmetry of the steel crack and boundary conditions, SIF of two tips were the same, thus either one could be used for analysis.

Eccentric crack (2a=10 mm; eccentricity ratio e0=30 mm) also had two tips; however, the SIF of two tips were different, thus the tip which was closer to the center was selected for analysis.

Edge crack (a=10 mm) extended in one direction, thus its tip was used for analysis.

One end of the steel plate was fixed, while simple tension was exerted upon the other end, σ=50 MPa.

Analytical solutions of the above three simple forms of cracks could be obtained through the equation $K_I = A\sigma\sqrt{\pi\alpha}$, where A refers to parameters related to crack positions and boundary conditions. Analytic formulas of above three kinds of cracks are as follows:

$$K_I = \sigma\sqrt{\pi\alpha} \tag{2.5}$$

$$K_I = 1.005\sigma\sqrt{\pi\alpha} \tag{2.6}$$

$$K_I = 1.3\sigma\sqrt{\pi\alpha} \tag{2.7}$$

According to the above analytic formulas, analytical solutions of the above three forms of cracks are shown in Table 1.

Table 1. Analytical solutions of cracks in three different forms

Crack form	Center crack	Eccentric crack	Edge crack
KI(MPa·mm0.5)	198	199	364

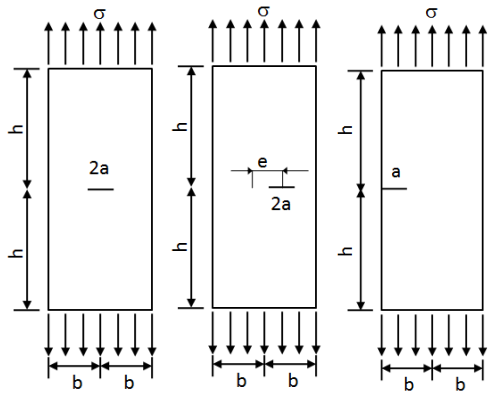

(a) Center crack (b) Eccentric crack (c) Edge crack

Fig. 1. Size of steel plates and crack positions

In analysis using ABAQUS, a two-dimensional model was selected, only its cross section was given solid property. Each kind of crack was analyzed using five different element types: linear quadrilateral elements (4-l), eight-node and other kinds of quadrilateral elements (4-q), quadrilateral singular elements (4-s), normal quadratic triangle elements (3-q) and degraded eight-node triangle singular elements (3-s). Specific mesh generation methods are shown in Fig. 2.

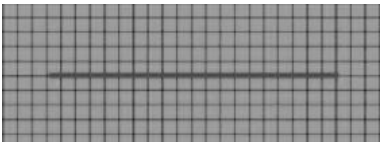

(a) Quadrilateral mesh

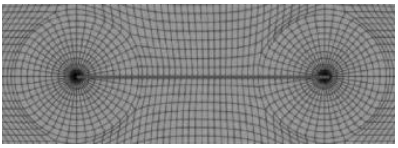

(b) Triangular mesh

Fig. 2. Different forms of mesh generation

2.2.2. CALCULATION PROCESS AND RESULT ANALYSIS

In this study, corresponding J-integral values were output and their SIF were calculated by ABAQUS software. One thing should be noted was that J-integral paths were loops surrounded the crack tip, and integrals were unrelated to paths but only related to the start point and the end point. In order to ensure the accuracy of calculation, 10 integral paths which surrounded the crack tip and extended outwards successively were set. Center crack 1 mm mesh was taken as an example and table 2 shows J values of different element types and integral paths. Table 2 shows that, the selected node of the first integral path was close to the crack tip, thus it was very unstable and significantly different from other values. However, as integral paths are away from the crack tip, J-integral values tended to be stable and uniform. The stable J-integral value in each group was selected and substituted into the formula $K_I = \sqrt{JE}$. Obtained K_I values after calculation were shown in Table 3.

Table 2. Calculation of J integrals of the center crack 1 mm mesh using Abaqus

Path	1	2	3	4	5	6	7	8	9	10	Stable value
4-l	1.243	1.456	1.485	1.493	1.498	1.499	1.498	1.498	1.498	1.498	1.498
4-q	1.475	1.486	1.488	1.488	1.488	1.488	1.488	1.488	1.488	1.488	1.488
4-s	1.510	1.499	1.492	1.484	1.478	1.468	1.462	1.452	1.444	1.436	1.428
3-q	1.432	1.490	1.492	1.492	1.492	1.492	1.492	1.492	1.492	1.492	1.492
3-s	1.501	1.501	1.502	1.502	1.502	1.502	1.502	1.502	1.502	1.502	1.502

Note: Unit of SIF in the table is $\mathrm{MPa}\bullet\sqrt{\mathrm{mm}}$; unit of J integral is MN/m.

Table 3. K_I results after J integral calculation

Center crack															
Mesh	0.5 mm					1 mm					2 mm				
Element	4-l	4-q	4-s	3-q	3-s	4-l	4-q	4-s	3-q	3-s	4-l	4-q	4-s	3-q	3-s
Analytical solution	686														
J integral	686	685	686	684	685	685	684	686	685	686	686	680	686	687	686
Off-centered crack															
Mesh	0.5 mm					1 mm					2 mm				
Element	4-l	4-q	4-s	3-q	3-s	4-l	4-q	4-s	3-q	3-s	4-l	4-q	4-s	3-q	3-s
Analytical solution	690														
J integral	689	687	389	688	689	690	387	689	686	689	689	688	683	690	389
Edge crack															
Mesh	0.5 mm					1 mm					2 mm				
Element	4-l	4-q	4-s	3-q	3-s	4-l	4-q	4-s	3-q	3-s	4-l	4-q	4-s	3-q	3-s
Analytical solution	892														
J integral	898	897	898	898	899	896	895	897	896	897	894	893	895	894	897

Note: Unit of the SIF in the table is $\mathrm{MPa}\bullet\sqrt{\mathrm{mm}}$; unit of J integral is MN/m.

Data in above tables show that, SIF obtained from J integral were stable and solutions obtained from different meshes and element types did not have excessive deviations. Besides, all solutions fluctuated

around analytical solutions on a small scale, which indicated high accuracy. Data comparison showed that the maximum deviation was only 1%.

3. SIMULATION OF FATIGUE CRACK GROWTH

3.1. EXTENDED FINITE ELEMENT METHOD

Current methods of fatigue crack simulation are varied, such as extended finite element method, fracture mechanics method and cohesive force model, etc. The extended finite element method is a new-type numerical method used to analyze discontinuous problems and its computational meshes are independent of all internal details. Thus, the extended finite element method is particularly suitable for analysis of crack growth problems. The extended finite element method has three characteristics: (1) internal physical or geometrical details are not taken into consideration in elements division; (2) other methods are used to determine the actual position of cracks and simulate crack growth; (3) based on existing knowledge of the studied problems, the extended finite element method can improve the shape function that influences intra-area elements, thus to reflect the existence and growth of cracks.

This study adopted the extended finite element method to simulate and calculate growth of different forms of cracks using ABAQUS software.

Description of the displacement field using traditional finite element method is based on elements. The displacement between elements can be congruous or incongruous; however, the displacement field $u^e(x)$ in every element is always expressed through the shape function Nek(x) and the element node displacement u_k:

$$u^e(x) = \sum_k N_k^e(x) u_k \tag{3.1}$$

where:

x – space coordinates and subscript k – nodes of elements.

In the extended finite element method, element edges are not always the crack surfaces, thus conventional element, penetrating crack element and crack tip element can be found in simulation. As shown in Fig. 3, the crack line passes through element 1, 2 and 3, thus element 1 and 2 are called

penetrating crack elements while element 3 is called the crack tip element; the remaining elements like elements 4 and 5 which are not passed through by the crack are called conventional elements.

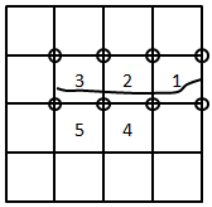

Fig. 3. Element division of extended finite element method

The following equation shows that, elements without cracks are conventional elements and element displacement is the first item of the equation. As for penetrating crack elements, the element displacement is the first two items of the equation. For crack-tip elements, the element displacement is the sum of the first and third item of the equation.

$$\begin{Bmatrix} u(x) \\ v(x) \end{Bmatrix} = \sum_{i\in I} N_i(x) \begin{Bmatrix} u_i \\ v_i \end{Bmatrix} + \sum_{j\in K_\Gamma \cap I} N_j(x) \begin{Bmatrix} \alpha_{ij} \\ \alpha_{2j} \end{Bmatrix} + \sum_{m\in K_\wedge \cap I} N_m \left(\sum_{l=1}^{4} \begin{pmatrix} c_{1k}^{l1} \\ c_{2k}^{l2} \end{pmatrix} B_l(x) \right) \tag{3.2}$$

In Eq. (3.2), Ni, Nj and Nm are shape functions of nodes; I refers to the set of nodes of all elements; $(u_i \quad v_i)^T$ is the continuous part of the displacement vector of nodes; $(\alpha_{ij} \quad \alpha_{2j})^T$ is the improved element degree of freedom of the part segmented by the crack; $(c_{1k}^{l1} \quad c_{2k}^{l2})^T$ is the improved degree of freedom of crack-tip elements; KΓ is the set of nodes of improved elements segmented by cracks (circles in the Fig. 3); $K_\wedge$ is the set of element nodes improved by the crack tip (small rectangles in the Fig. 3).

Methods used for determination of the specific location of the crack are varied, and a commonly used method is the level set method (LSM) which was put forward by Osher and Sethian and used to determine crack location as well as track crack growth [20]. In ABAQUS software, the most commonly used method to simulate growth process of cracks is the extended finite element method. On the basis of theories of the extended finite element method, singular elements are not required for the crack tip, and mesh division is simple. The wire feature method is used to simulate cracks of plane crack models [21].

3.2. EXTENDED FINITE ELEMENT METHOD

Traffic load is an important parameter in analyzing the mechanism of fatigue crack growth of steel bridge structures. On the basis of the finite element model updating, low pass filter and multi-girder vehicle-bridge coupled vibration program, this study put forward a method of recognizing moving loads of multi-girder bridge based on the finite element model updating. In such recognition method, dynamic responses of the passing vehicles are given filtering processing to eliminate the influence from impact of vehicle-bridge interaction, vehicle suspension system parameters, vehicle types and driving speed of the vehicle, etc. Secondly, finite element models are updated on the basis of static test data, and the bridge system is given preliminary calibration, thus to improve the accuracy of load identification. After that, updated finite element model of the bridge is input into the multi-girder vehicle-bridge coupled vibration program. Taking the static force extreme value after filtering as the analysis object, horizontal positions and vehicle weight parameters of the passing vehicles are recognized according to the vehicle type classification, and vehicle weight parameters are statistically analyzed. The flow chart of recognition is shown in Fig. 4.

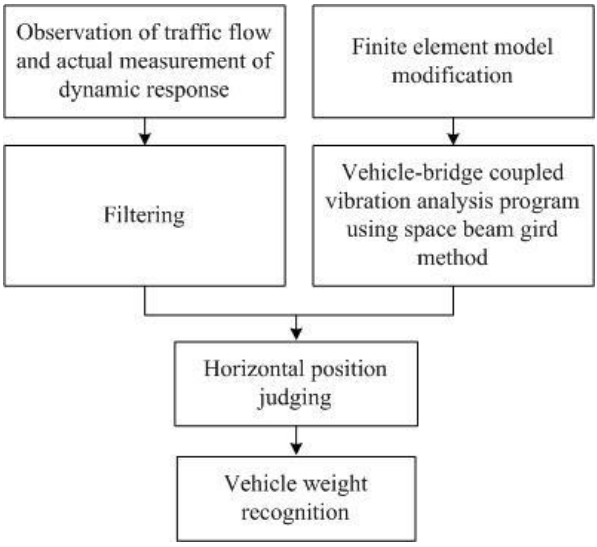

Fig. 4. Flow chart of recognition of vehicle weight parameters

3.3. Simulation of crack growth paths under different loads

Stress is the decisive factor of crack growth directions. For mixed-mode cracks which contain two or more than two crack types, such as I – II mixed-mode cracks, changes of growth paths under the tangential stress should be considered. The model shown in figure 5 was used in this study. The original angle of the crack was designed as 0° ; tensile stress 10MPa, 20MPa and 40MPa as well as tangential stress 40MPa was applied to the model. Three groups of models were built and calculation results were compared. Tensile stress 10MPa, 20MPa and 40MPa corresponded to the model number one, model number two and model number three respectively; crack growth paths of the three models under different loads are shown in Fig. 6.

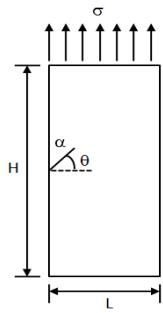

Fig. 5. Crack growth model

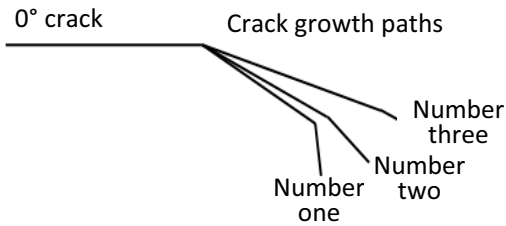

Fig. 6. Crack growth paths of three models

On the basis of above crack models, the initial angle of the crack was designed as 45° and the load was changed. The number one path: only 80MPa tensile stress was exerted on the vertical top surface. The number two path: tensile stress and 40MPa right shearing stress of the top surface were exerted simultaneously. Crack growth paths are shown in Fig. 7.

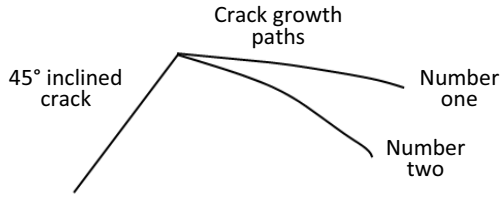

Fig. 7. Comparison of growth paths of the crack in 45° dip angle under different loads

Fig. 6 and Fig. 7 show that the effect of loads on crack growth paths is significant. The crack growth path is approximately vertical to the load line under the tensile stress, while the crack extends downwards under tangential stress. The simulation results were similar to the mechanics principles, which verified the reliability of such simulation method.

4. CASE STUDY

4.1. EXPERIMENTAL OBJECT AND METHODS

Sutong Bridge was selected as the research object in this study and a part of the bridge was used for calculation. The average natural vibration period of the cable bent tower of Sutong Bridge is between 5.3 s and 10.2 s, while the natural vibration frequency is 0.09-0.2 Hz. Calculation models included a hole-dug diaphragm plate and two vertical U-shape girders. According to the on-spot experiment and observation, some parts of the bridge already had cracks due to the vehicle loads accumulated over a long period of time. Because only a partial model was selected in this study, cracks were designated according to stress features instead of copying crack positions; crack growth paths were simulated using the extended finite element method in this study. Details about the model are shown in Fig. 8.

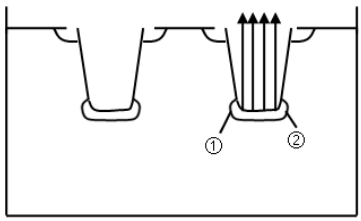

Fig. 8. Partial model of the Sutong Bridge

Boundary conditions of the partial model can be different from that of the whole model, thus the rigid body displacement of the selected partial model should be restricted during calculation. Besides, load was added on one U-shape girder to simulate the vehicle load. As shown in figure 6, load was added on the second U-shape girder, thus the girder bore big stress and was most likely to have cracks. Therefore, two original cracks were simulated in the girder for analysis. Specific data of the load were as follows: pressure of the vehicle was 550 kN; the touchdown length of the tire was 1.8 m; width of the tire was 0.4 m; thickness of covering soil of culvert was 3 m and the actual stress was about 78 Mpa.

Using the extended finite element program that came with the ABAQUS software, main works focused on setting material parameters. The research object in this study was steel structures, thus except the basic mechanics parameters like elasticity modulus and Poisson ratio, other parameters like fracture criteria, damage evolution and fracture toughness should also be determined. In addition, the extended finite element method is not suitable for shell elements, thus models should be built according to solid elements. Large deformation of the structure can occur in calculation which is not easy to converge, thus conditions of convergence should be relaxed and added loads should be in the displacement form.

4.2. Calculation results

4.2.1. Simulation of crack growth paths

Crack growth paths can be simulated rapidly and directly using the extended finite element method and only early modeling procedures are needed during the process to get results. Figure 9 shows the growth tendency of the crack, and the growth of the crack does not cling to meshes, which verified the advantage of the extended finite element that meshes can not be redistricted.

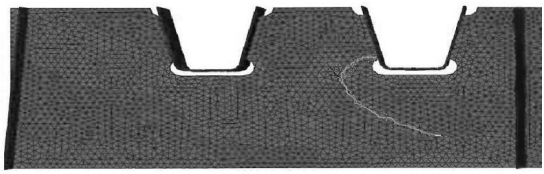

(a) Growth path of crack ①

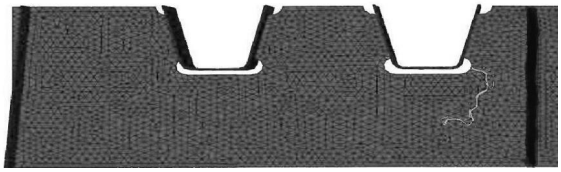

(b) Growth path of crack ②

Fig. 9. Crack growth paths obtained with extended finite element method

4.2.2. EFFECT OF MESH SIZE ON THE GROWTH PATH OF CRACK

Traditional finite element calculation methods were usually based on the mesh partition. This study also explored the effect of different mesh sizes on calculation results using the extended finite element method, as shown in Fig. 10.

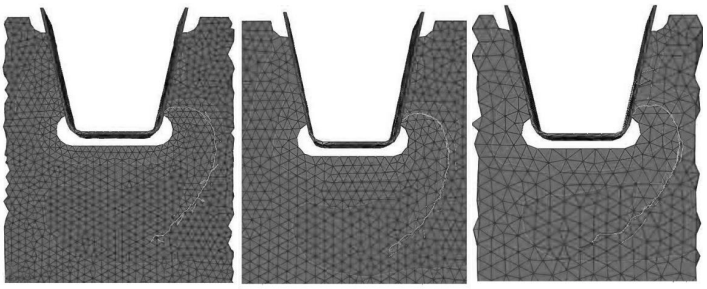

(a) 15mm mesh (b) 20mm mesh (c) 35mm mesh

Fig. 10. Growth paths of crack ②using girds in different sizes

Figure 10 further verified that no effect of mesh size was found on growth paths of cracks; crack growth paths and stress distribution were exactly the same in girds in three different sizes.

5. CONCLUSION

This study introduces the J-integral method and the extended finite element method. Experiment results indicate that the J-integral method has wide application and it has no specific requirements on element types and mesh sizes, thus it has high efficiency. More importantly, the J-integral method can

meet the accuracy requirement better and its error is within 1%. The new extended finite element method in ABAQUS software is used to predict crack growth paths and good results are obtained. Following conclusions are obtained: the application of the extended finite element method is not directly related to mesh sizes, and crack growth paths simulated by mesh in different sizes are exactly the same; the extended element method stringently follows the mixed-mode fracture criteria, thus the obtained results are reliable. Therefore, the extended finite element method can be widely applied to engineering practices because it is highly effective, reliable and worthy of being widely promoted.

REFERENCES

1. L. Reid. "Repairing and preserving bridge and steel structure using an innovative crack arrest repair system", Advanced Materials Research, 891-892:1217-1222, 2014.
2. H. Y. Lee, J. B. Kim, W. G. Kim, et al. "Creep-fatigue crack behaviour of a mod. 9Cr1Mo steel structure with weldments", Transactions of the Indian Institute of Metals 63(2):245-250, 2010.
3. E. Sgambitterra, S. Lesci, C. Maletta. "Effects of higher order terms in fracture mechanics of shape memory alloys bydigital image correlation", Procedia Engineering, 109:457-464, 2015.
4. J. M. L. Reis. "Sisal fiber polymer mortar composites: Introductory fracture mechanics approach", Construction & Building Materials, 37(37):177-180, 2012.
5. R. Wang, A. Nussbaumer. "Modelling fatigue crack propagation of a cracked metallic member reinforced by composite patches", Engineering Fracture Mechanics 76(9):1277–1287, 2009.
6. X. Q. Feng, Y. F. Shi, X. Y. Wang, et al. "Dislocation-based semi-analytical method for calculating stress intensity factors of cracks: Two-dimensional cases", Engineering Fracture Mechanics, 77(18):3521-3531, 2010.
7. Y. D. Li, Y. L. Kang, Z. Nan. "Dynamic stress intensity factor of a crack perpendicular to the weak-discontinuous interface in a nonhomogeneous coating–substrate structure", Archive of Applied Mechanics, 79(2):175-187, 2009.
8. G. Meneghetti, C. Guzzella. "The peak stress method to estimate the mode I notch stress intensity factor in welded joints using three-dimensional finite element models", Engineering Fracture Mechanics, 115(1):154-171, 2014.
9. W. Zhang. "Calculation of dynamic stress intensity factor by the boundary element - laplace transform method", Advanced Materials Research, 989-994:1825-1828, 2014.
10. P. V. Jogdand, K. S. R. K. Murthy. "A finite element based interior collocation method for the computation of stress intensity factors and T-stresses", Engineering Fracture Mechanics, 77(7):1116-1127, 2010.
11. N. H. Dao, H. Sellami. "Stress intensity factors and fatigue growth of a surface crack in a drill pipe during rotary drilling operation", Engineering Fracture Mechanics, 296:626-640, 2012.
12. Y. U. Dazhao. "Stress intensity factor of cracks in bolted joints based on three-dimensional finite element analysis", Journal of Mechanical Engineering, 47(20):121-126, 2011.
13. A. O. Ayhan. "Three-dimensional fracture analysis using tetrahedral enriched elements and fully unstructured mesh", International Journal of Solids and Structures, 48(3):492-505, 2011.
14. Y. Peng, L. Tong, X. L. Zhao., et al. "Modified stress intensity factor equations for semi-elliptical surface cracks in finite thickness and width plates", Procedia Engineering, 14:2601-2608, 2011.
15. N. Sukumar, D. L. Chopp, B. Moran. "Extended finite element method and fast marching method for three-dimensional fatigue crack propagation", Engineering Fracture Mechanics, 70(1):29-48, 2003.
16. A. Đurđević, D. Živojinović, A. Grbović, et al. "Numerical simulation of fatigue crack propagation in friction stir welded joint made of Al 2024T351 alloy", Engineering Failure Analysis, 58:477-484, 2015.
17. Y. Prawoto, I. H. Onn. "Application of J-integral concept on blister coating problem", Engineering Fracture Mechanics, 92:114–125, 2012.
18. J. Liu, M. Coret, A. Combescure, et al. "J-integral based fracture toughness of 15Cr–5Ni stainless steel during phase transformation", Engineering Fracture Mechanics, 96:328–339, 2012.
19. E. Giner, N. Sukumar, J. E. Tarancon, et al. "An Abaqus implementation of the extended finite element method", Engineering fracture mechanics, 76(3):347-368, 2009.

20. L. Chunming, H. Rui, D. Zhaohua, et al. “A level set method for image segmentation in the presence of intensity inhomogeneities with application to MRI”, IEEE Transactions on Image Processing A Publication of the IEEE Signal Processing Society, 20(7):2007-2016, 2011.
21. Y. B. Kar, N. A. Talik, Z. Sauli, et al. “Finite element analysis of thermal distributions of solder ball in flip chip ball grid array using ABAQUS”, Microelectronics International, 30(1):14-18, 2013.

Received 10.03.2016

Revised 03.05.2016

LIST OF FIGURES AND TABLES:

Fig. 1. Size of steel plates and crack positions

Rys. 1. Rozmiar płytek stalowych i pozycje pęknięć

Fig. 2. Different forms of mesh generation

Rys. 2. Różne formy generowania siatki

Fig. 3. Element division of extended finite element method

Rys. 3. Podział elementów rozszerzonej metody elementów skończonych

Fig. 4. Flow chart of recognition of vehicle weight parameters

Rys. 4. Diagram rozpoznawania parametrów wagi pojazdów

Fig. 5. Crack growth model

Rys. 5. Model rozwoju pęknięć

Fig. 6. Crack growth paths of three models

Rys. 6. Ścieżki rozwoju pęknięć trzech modeli

Fig. 7. Comparison of growth paths of the crack in 45° dip angle under different loads

Rys. 7. Porównanie ścieżek rozwoju pęknięć pod kątem 45° przy różnych obciążeniach

Fig. 8. Partial model of the Sutong Bridge

Rys. 8. Częściowy model mostu „Sutong”

Fig. 9. Crack growth paths obtained with extended finite element method

Fig. 10. Growth paths of crack ②using girds in different sizes

Rys.10 dalej zweryfikowano brak wpływu rozmiaru siatki na ścieżki rozwoju pęknięć; ścieżki rozwoju pęknięć i dystrybucja naprężenia były identyczne w siatkach 3 różnych rozmiarów.

Tab. 1. Analytical solutions of cracks in three different forms

Tab. 1. Analityczne rozwiązania pęknięć w różnych formach

Tab. 2. Calculation of J integrals of the center crack 1 mm mesh using Abaqus

Tab. 2. Obliczanie pęknięcia środkowego przy siatce 1 mm według całki J przy wykorzystaniu programu Abaqus

Tab. 3. K_1 results after J integral calculation

Tab. 3. Wyniki KI po obliczeniu całki J

MECHANIZM ROZWOJU PĘKNIĘĆ ZMĘCZENIOWYCH STALOWYCH KONSTRUKCJI MOSTÓW

Słowa kluczowe: czynnik intensywności naprężenia; rozszerzona metoda elementów skończonych; symulacja rozwoju pęknięć zmęczeniowych; most

STRESZCZENIE:

Ostatnimi laty, wraz z gwałtownym rozwojem chińskiego przemysłu transportowego, budowa mostów w Chinach weszła w nowy etap rozwoju robiąc duży krok naprzód i coraz więcej mostów rzecznych i morskich wyrasta z ziemi, a mosty te stały się niezastąpioną osią chińskiej sieci transportowej. Konstrukcja stalowa jest głównym komponentem budowy mostu; jednakże, może ulec zniszczeniu poprzez ciągłe obciążanie doprowadzając w ten sposób do pęknięć zmęczeniowych. Wraz ze wzrostem budowy mostów zwiększa się liczba fatalnych wypadków spowodowanych pęknięciami zmęczeniowymi, prowadząc do wysokich praktycznych wymagań dotyczących bezpieczeństwa i niezawodności konstrukcji.

Współczynnik intensywności naprężenia (WIN) i kryteria rozwoju pęknięć to dwa kluczowe problemy w mechanice pęknięć. Metody obliczania WIN obejmują metodę analityczną i numeryczną, przy czym numeryczna metoda obejmuje metodę elementów skończonych, metodę objętości skończonej oraz metodę elementów brzegowych itd. Metoda elementów skończonych jest najczęściej stosowana do obliczania WIN, a metody obliczania WIN obejmują metodę zależną od przemieszczeń, wirtualną metodę zamykania szczelin, metodę całki J itd. Teoretyczny proces dedukcji WIN jest skomplikowany. Dla różnych modeli pęknięć zmiany warunków brzegowych spowodują brak przydatności pierwotnej metody obliczeniowej, tak więc należy wydedukować nową metodę obliczeniową. Dlatego symulacja elementów skończonych jest obecnie szeroko stosowana do modelowania obliczeń różnych modeli, ponieważ może znacząco skrócić czas tradycyjnych obliczeń, jak również poprawić ich wydajność.

Na podstawie mechaniki pękania przestudiowano WIN oraz ścieżki rozwoju pęknięć biorąc za przykład model mostu „Sutong", zasymulowano małe pęknięcia na dwóch niebezpiecznych częściach mostu oraz zastosowano obciążenie pojazdem względem ceownika, aby przewidzieć ścieżki rozwoju pęknięć. Wyciągnięto następujące wnioski:

(1) Obliczanie WIN przy użyciu metody całki J

W tej pracy zastosowano metodę całki J. Na podstawie formuły obliczeniowej całki J jak również na podstawie analizy elementów skończonych opartej o program „abakus" przeanalizowano odpowiednio płytki stalowe z pęknięciem centralnym, z pęknięciem mimośrodowym i z pęknięciem brzegowym. Dodatkowo, aby zweryfikować wpływ typów elementów i rozmiary siatki na wyniki obliczeń, każdy typ pęknięcia został przeanalizowany przy użyciu pięciu różnych typów elementów i można z tego wywnioskować, że metoda całki J wykazała się wysoką precyzją i była łatwa w obsłudze. Wartości WIN na podstawie metody całki J były stabilne, a różnice w wynikach różnych rozmiarów siatki i różnych typów elementów nie były istotne. Tak więc metoda całki J miała dużą dokładność. Największe odchylenie wartości wynosiło tylko 1%. Z wyjątkiem stabilności, metoda całki J jest również bardzo wygodna. Oprogramowanie abaqus może bezpośrednio podać wartości całki J, a co za tym idzie, może być obliczana według otrzymywanych stabilnych wartości.

(2) Symulacja rozwoju pęknięć zmęczeniowych

Przewidywane ścieżki rozwoju pęknięcia zostały przeanalizowane w niniejszej pracy przy wykorzystaniu rozszerzonej metody elementów skończonych. Przeanalizowano również podstawowe teorie, charakterystyki i warunki zastosowania rozszerzonej metody elementów skończonych, rozpoznanie obciążenia mostu ruchem i symulację rozwoju ścieżek pęknięć przy różnych obciążeniach. Aby przewidzieć ścieżki rozwoju pęknięcia opracowano model pęknięcia pochylonego pod kątem 45° i zastosowano rozszerzoną metodę elementów skończonych. Sprawdzono, że wyniki symulacji były takie same jak wyniki obliczeń przy zastosowaniu metody elementów skończonych, która zweryfikowała dokładność mechanizmów pęknięć jak również symulację przy wykorzystaniu rozszerzonej metody elementów skończonych.

(3) Przykładowa analiza oparta na moście „Sutong”

Jako przykład został wykorzystany most rzeczny „Sutong” łączący miasta Suzhou i Nantong w chińskiej prowincji Jiangsu y. Modele obliczeniowe mostu „Sutong” obejmowały płytę membrany wykopu i dwa podłużne ceowniki; według charakterystyki naprężenia wybrano kilka pęknięć i zastosowano rozszerzoną metodę elementów skończonych, aby zasymulować ścieżki rozwoju pęknięć. Wyniki obliczeń wykazały, że zastosowanie rozszerzonej metody elementów skończonych różnych rozmiarów siatki były identyczne; rozszerzona metoda elementów skończonych została przeprowadzona dokładnie według kryterium pęknięć trybu mieszanego, a otrzymane wyniki były wiarygodne. Dlatego rozszerzona metoda elementów skończonych może być szeroko stosowana do zastosowań inżynieryjnych i jest godna polecenia oraz powinna być szeroko upowszechniana.